Subtidal inner-shelf circulation near Point Conception, California

Cynthia N. Cudaback
Department of Marine, Earth and Atmospheric Sciences, North Carolina State University, Raleigh, North Carolina, USA

Libe Washburn
Institute for Computational Earth Systems Science, University of California, Santa Barbara, California, USA

Ed Dever
College of Oceanic and Atmospheric Sciences, Oregon State University, Corvallis, Oregon, USA

Received 19 July 2004; revised 7 March 2005; accepted 29 April 2005; published 8 October 2005.

[1] We discuss connections between inner-shelf and mid-shelf circulation near Point Conception, California, as well as the wind forcing of inner-shelf circulation. Point Conception marks the southern edge of a major upwelling zone that extends from Oregon to central California. The coastline makes a sharp eastward turn at Point Conception, and the Santa Barbara Channel to the east is generally assumed to be an upwelling shadow. Consistent with this regional division, inner-shelf currents are strongly correlated with wind north of Point Conception, but not in the Santa Barbara Channel. One exception to this generalization is a location in the Santa Barbara Channel, near a pass that cuts through the coastal mountains, where local winds have a dominant cross-shore component and directly drive cross-shore currents over the inner shelf. Inner-shelf currents in the Santa Barbara Channel, when compared with mid-shelf currents in that area, are weaker, but strongly correlated. By contrast, inner-shelf currents north of Point Conception show a far greater incidence of poleward flow than is seen over the mid-shelf in that area. Poleward flow events, lasting 1–5 days, transport warm water from the Santa Barbara Channel around Point Conception to the central California coast. These events are associated with relaxation of the generally equatorward wind, but not always with mid-shelf flow reversals.

Citation: Cudaback, C. N., L. Washburn, and E. Dever (2005), Subtidal inner-shelf circulation near Point Conception, California, *J. Geophys. Res.*, *110*, C10007, doi:10.1029/2004JC002608.

1. Introduction

[2] The inner shelf, lying between the surf zone and the horizon, was once considered "too shallow for oceanographers with ships, too deep for coastal engineers without ships" [*Smith*, 1995]. This interesting region has received much more attention in the last 10 years. Most studies of the inner shelf have focused on defining it and on understanding its wind- and wave-driven dynamics, generally in the context of coastal upwelling [*Lentz*, 1995; *Austin and Lentz*, 2002]. Prior to this study, less work has been done on the connections between the inner and mid-shelf.

[3] The inner shelf is usually defined in terms of upwelling dynamics. Classical upwelling theory predicts cross-shelf transport proportional to the wind stress. This prediction applies only if the surface and bottom boundary layers do not overlap, and so is valid over the mid-shelf and outer shelf. Over the inner shelf, overlapping boundary layers cause reduced cross-shelf transport relative to the mid-shelf; the resultant cross-shelf divergence of transport drives upwelling [*Lentz*, 1995; *Austin and Lentz*, 2002]. Thus the inner shelf is the region of reduced cross-shelf transport [*Lentz*, 1995], and also the region inshore of the upwelling front [*Austin and Lentz*, 2002]. The dynamic definition of the inner shelf means its spatial extent is a function of surface stress, bottom stress, stratification, and surface wave variation. At midlatitudes and for moderate wind speeds, the inner shelf has a depth of less than 60–100 m.

[4] Density stratification over the inner shelf can decouple the boundary layers, allowing strong cross-shore transport. Most prior studies, as well as the present study, are in areas where thermal stratification dominates. *Lentz* [2001] measured cross-shelf transport on the North Carolina coast during a time of changing stratification. When the top to bottom temperature difference was 10°C, observed transport equaled Ekman transport, but the transport reduced significantly after a passing storm destratified the water column. Over the New Jersey shelf, Ekman transport was observed with a surface to bottom temperature difference of 4–14°C (data provided by A. Muenchow). By contrast, the vertical temperature difference over the central California inner

0148-0227/05/2004JC002608$09.00

shelf is only 2–5°C. In this region observed cross-shelf transport is about 25% of Ekman's prediction [*Lentz*, 1994], and subtidal along-shelf current speeds are about 40% of the mid-shelf currents [*Lentz*, 1994].

[5] Existing studies have generally focused only on the inner shelf, not on the connections between inner-shelf and mid-shelf processes, but these connections may be of vital importance to the shore. Over scales of tens to thousands of kilometers, the motions of oil spills, bath toys, and the larvae of fish and invertebrates depend on coastal and ocean-scale circulation [*Ebbesmeyer and Ingraham*, 1994; *Dever et al.*, 1998; *Gaylord and Gaines*, 2000]. However, transport over the inner shelf determines whether a given object actually hits the beach and may significantly affect our perceptions of larger scale processes. Transport along the inner shelf may also have a significant effect on nearshore ecosystems [*Pineda*, 2000]. For these reasons, studying inner-shelf circulation is a primary objective for the Partnership for Interdisciplinary Studies of the Coastal Ocean (PISCO) project (http://www.piscoweb.org/).

1.1. Circulation Around Point Conception

[6] The southern PISCO study site extends from the western Santa Barbara Channel (SBC), around Point Conception and northward into the Santa Maria Basin (SMB). Point Conception (PtC) marks the southern edge of the California-Oregon upwelling zone, and is a major bio-geographic boundary [*Valentine*, 1966; *Wares et al.*, 2000]. North of PtC, the coastline runs north-south, exposed to the prevailing southeastward winds (20–40 knots [*Dorman and Winant*, 2000]). At Point Conception, the coastline turns sharply eastward into the SBC. The east-west running Santa Ynez mountains block the wind, allowing calm conditions in the SBC, and the lack of upwelling means that the water in the SBC is often significantly warmer than the SMB. Local fishermen refer to the southern waters as "God's country" [*de Santis*, 1985].

[7] This region has been the site of several prior observational programs that have focused on the shelf and basin-wide circulation. Upwelling at Point Conception can deliver materials into the Santa Barbara Channel or export them offshore [*Atkinson et al.*, 1986; *Barth and Brink*, 1987]. In the Santa Maria Basin, circulation is correlated with the strong local wind forcing [*Strub et al.*, 1987]. By contrast, within the SBC, there is strong spatial variability in the direction and strength of the wind, and circulation is not always well correlated with the local wind forcing [*Brink and Muench*, 1986]. More recent studies have described synoptic states that capture the variability in mid-shelf circulation [*Harms and Winant*, 1998; *Winant et al.*, 2003; *Dever*, 2004].

[8] Winds near Point Conception are generally southward both winter and summer, in contrast with the seasonally reversing winds over the Northern California shelf [*Strub et al.*, 1987]. Equatorward winds are generally opposed by an along-shore pressure gradient, and the relative strength of the two forces determines the coastal circulation patterns in the area [*Dorman and Winant*, 2000; *Muenchow*, 2000; *Oey et al.*, 2001]. North of Point Conception, the winds roughly parallel the coast, and upwelling dominates the circulation. At Point Conception, the coastline turns sharply eastward and winds separate from the shore. The spatial gradients in wind stress and the pressure gradient force combine to drive counterclockwise circulation in the Santa Barbara Channel [e.g., *Hendershott and Winant*, 1996; *Auad and Hendershott*, 1997; *Harms and Winant*, 1998; *Dever et al.*, 1998; *Dorman and Winant*, 2000; *Winant et al.*, 2003; *Dever*, 2004]. The bend in the coastline creates these two distinct regions in coastal circulation, and may significantly affect inner-shelf circulation as well.

[9] The time-averaged picture above is subject to significant seasonal variations, with three basic circulation states [*Dever et al.*, 1998; *Dever*, 2004]. The convergent state is defined by southward currents in the SMB and westward currents on the north side of the SBC [*Dever et al.*, 1998]. This circulation pattern, which also includes a strong cyclonic circulation in the channel, is dominant in late summer, when a strong pressure gradient drives poleward currents on the north side of the channel. The upwelling state is defined by equatorward currents in the SMB and SBC. This circulation pattern dominates in spring, when the winds are strong and the pressure gradient is weak. The relaxation state is defined by poleward currents on both sides of Point Conception; the currents diverge from the coast at the point [*Dever*, 2004]. This circulation pattern is short lived, but can occur at any time of the year. Relaxation events are driven by winter storms and are also observed in summer, when the pressure gradient is strong and the winds weak, owing to relaxation of the dominant equatorward winds.

1.2. Goals

[10] The overall goal of the present work is to interpret the inner-shelf circulation near Point Conception in view of larger-scale synoptic processes. Specific goals are (1) to compare new measurements of inner-shelf circulation near Point Conception with previous descriptions of mid-shelf circulation, (2) to assess the effects of regional and local winds on inner-shelf circulation, and (3) to determine the effects of inner- and mid-shelf circulation on inner-shelf temperature variability.

2. Methods

2.1. Observations

[11] To investigate the dynamics of the inner shelf around Point Conception, moored thermistors and bottom-mounted acoustic Doppler current profilers (ADCPs) were deployed at six locations, as part of the PISCO project. The mooring-ADCP pairs were deployed on either side of Point Conception at 15- to 20-km intervals, nominally along the 15-m isobath (Figure 1). The moorings and ADCPs were initially deployed between June 1999 and June 2000 and were still in operation as of early 2004.

[12] Moorings were equipped with thermistors ("Tidbit" models, made by Onset Corporation, Bourne, MA.) at depths of 3, 9, and 14 m. They recorded temperature every 2 min with an absolute accuracy of 0.2°C, resolution of 0.16°C, and a 3-min response time. The ADCPs (600-kHz "workhorse" model manufactured by R. D. Instruments, San Diego, California) were bottom mounted, looking upward; this configuration prevents effects of sensor

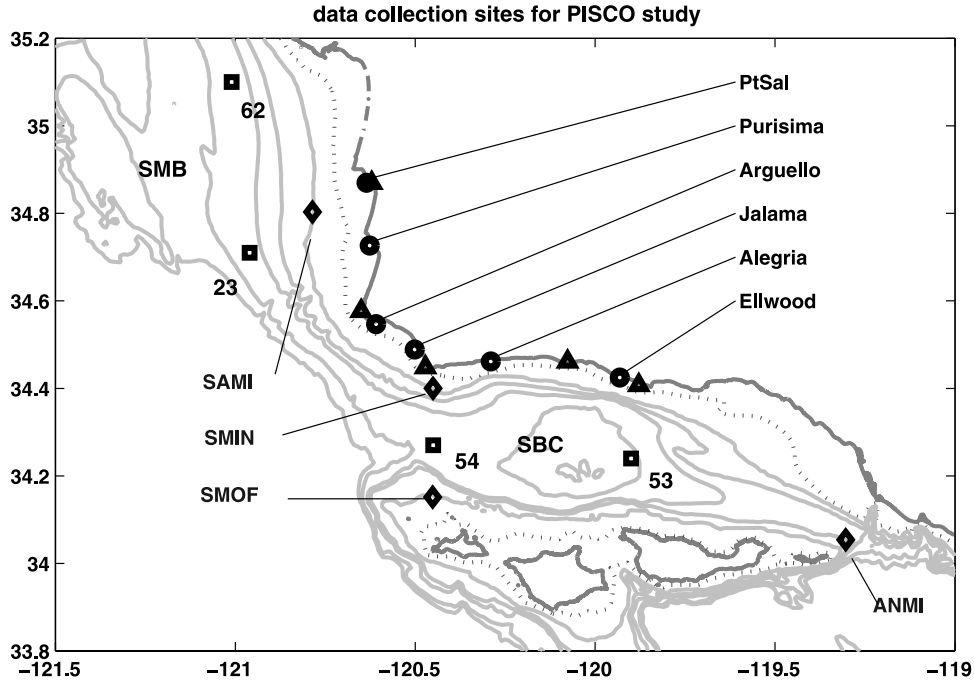

Figure 1. Locations of PISCO inner-shelf moorings (circles), NDBC moorings (squares; mooring numbers all start with 460, last 2 digits are shown) SIO moorings (diamonds), and HF radar land stations (unlabeled triangles). Point Conception is just north of mooring SMIN. Bathymetric contours are marked for 50-m (dotted line) and 100-m intervals (solid lines). SBC and SMB are the Santa Barbara Channel and Santa Maria Basin, respectively.

motion, such as can occur with moored ADCPs. Currents were measured throughout the water column every 2 min, with a vertical resolution (bin size) of 1 m. Temperature and velocity time series were low-pass filtered to remove fluctuations on timescales of 40 hours and shorter (PL64 filter, described by *Limeburner* [1985]).

[13] These data were augmented with hourly maps of surface currents (about 1 m depth) from a land-based network of up to five high-frequency (HF) radars, manufactured by CODAR Ocean Sensors, Ltd., Los Altos, California. The HF radars produced spatial averages of currents over circles of 3 km radius, using the method of *Gurgel* [1994]. Surface current vectors were interpolated onto a square grid with 2 km spacing. Further details on the performance, configuration and results of the radar network are described by *Beckenbach and Washburn* [2004] and *Emery et al.* [2004].

[14] Currents were measured at four locations in the SMB and SBC by the Center for Coastal Studies of the Scripps Institution of Oceanography (SIO). Moorings SAMI, SMIN, SMOF, and ANMI were located over the mid-shelf, on the 100-m isobath (diamonds, Figure 1). Mid-shelf current time series at 5 m depth from 1994 through 2003 were used in this analysis.

[15] We also analyzed wind and sea-surface temperature data from meteorological buoys maintained by NOAA's National Data Buoy Center (squares, Figure 1). Wind data from a shore-based station at Purisima in the SMB were provided by SIO, and meteorological data from the north shore of the SBC were provided by the Santa Barbara County Air Pollution Control District (SBAPCD). Wind stress was calculated using a neutral drag coefficient [*Large and Pond*, 1981].

2.2. Data Analysis

[16] Currents over the mid-shelf and inner shelf were averaged both over the entire deployment time of each instrument and using the conditional averaging method of *Dever* [2004]. The SIO moorings were used to identify times when regional synoptic flow states occurred. The upwelling, or equatorward flow state consists of southward currents at SAMI and eastward currents at ANMI. The convergent flow state consists of southward currents at SAMI and westward currents at ANMI. The relaxation, or poleward flow state consists of northward currents at SAMI and westward currents at ANMI.

[17] Conditional averaging was used in two different ways. First, long-term average currents were calculated for each condition, using 7 years of SIO observations (at SAMI and SMIN), 4 years of HF radar data, and nearly 5 years of ADCP data from the inner shelf. These average flow vectors are shown in section 3.1. Second, current data from the SIO moorings were run through a 3-week low-pass filter and used to calculate a running index of flow conditions. Three-week low-passed wind speeds from NDBC Buoy 46062 were color coded according to flow condition for the time series plot in section 3.2.

[18] The relationship between inner-shelf currents and wind was examined using an empirical orthogonal function (EOF) analysis of depth-dependent currents (section 3.4). We consider the principal axis (alongshore and poleward at each station) and cross-principal axis (cross-shore) compo-

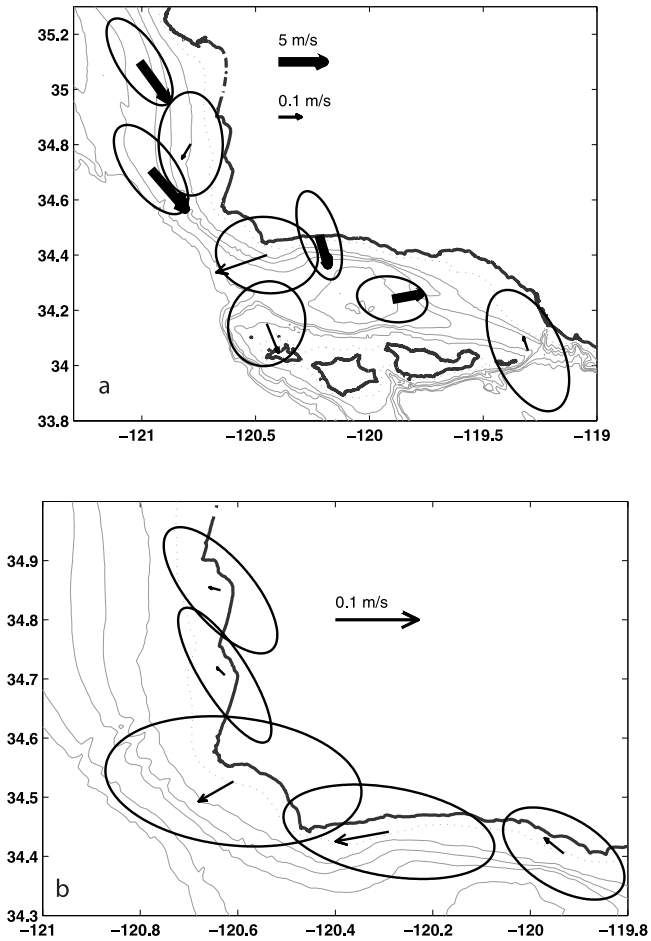

Figure 2. (a) Mean and principal axis winds (thick arrows) and mean and principal axis currents, measured 5 m below the surface, from SIO moorings. (b) Inner-shelf currents 2 m below surface, from PISCO ADCP data. Inner-shelf current vectors are shown slightly south of their true locations.

nents separately in the time series analysis. The correlations between wind speed and the first EOF of each velocity component were calculated every hour, using a 30-day interval centered on that hour. The 30-day interval was chosen as a compromise between temporal resolution and degrees of freedom. On the basis of a 30-day correlation interval and a 2-day auto-decorrelation time for winds [*Dorman and Winant*, 2000], each correlation contains 15 independent samples, giving a 95% confidence threshold of $r^2 = 0.26$.

3. Results

[19] Our observations reveal similarities and dissimilarities between mid-shelf and inner-shelf circulations. In the Santa Barbara Channel, we compare currents over the inner shelf at Alegria with currents over the nearest mid-shelf mooring, SAMI. The two time series are strongly correlated, and show the same seasonal variability. By contrast, in the Santa Maria Basin, the inner shelf experiences much more poleward flow than does the mid-shelf. Poleward flow events occur over the inner shelf even during the "upwelling" state defined using the SIO moorings [*Dever*, 2004].

3.1. Inner-Shelf Response to Coastal Circulation States

[20] We compare new measurements of inner-shelf currents with previously reported mid-shelf currents and winds, using the mean vectors and principal axes of variability. Average winds throughout our study area are equatorward and favorable to upwelling (Figure 2a). Winds at NDBC buoys 46062 and 46023, in the Santa Maria Basin, are strongly correlated ($r^2 = 0.94$). At each buoy, the principal axis of variability (313–319 true) is nearly parallel to the mean wind direction, and the eccentricity of the variance ellipse indicates that winds tend to reverse with little rotation. The high correlation between winds at different locations in the SMB allows us to use the most complete data time series, collected at NDBC buoy 46062, for the analyses in Sections 3.2 and 3.4.

[21] The east-west running Santa Ynez mountain range shelters the Santa Barbara Channel from strong southeastward winds. Winds in the eastern Channel (e.g., at NDBC buoy 46053) are therefore weaker and less correlated with winds in the SMB ($r^2 \approx 0.25$). Winds on the north shore of the channel are spatially incoherent and generally weak and variable. The one exception is on the coast south of Gaviota Pass, near mooring Alegria, where mean winds are strongly southward (Figure 2). At this location only, the principal axis of variability of the wind is nearly perpendicular to the coast. Gaviota winds are significantly correlated with principal axis winds at NDBC buoy 46023 ($r^2 = 0.52$), although the wind directions are different.

[22] Mean currents over the mid-shelf are equatorward in the SMB, offshore near Point Conception, and poleward in the eastern SBC. The mean currents at moorings SAMI, SMIN, SMOF, and ANMI (Figure 2a) are thus consistent with the cyclonic eddy and the convergent flow state described in prior studies [e.g., *Hendershott and Winant*, 1996; *Auad and Hendershott*, 1997; *Harms and Winant*, 1998; *Dever et al.*, 1998; *Dorman and Winant*, 2000; *Winant et al.*, 2003; *Dever*, 2004]. The variance ellipses are less eccentric for the currents than for the wind, indicating that currents are highly variable in speed and direction.

[23] By contrast with the mid-shelf, mean currents over the inner shelf are poleward in the SBC and SMB (Figure 2b, currents from Jalama not shown). In the SBC, at Alegria and Ellwood, mean currents and the principal axis of variability closely follow the local bathymetry. Mean currents in the SMB are somewhat weaker, and also parallel to the local bathymetry. Near Point Conception, mean inner-shelf currents have a distinct offshore component, parallel to mean currents over the mid-shelf (Figure 2a). This is consistent with upwelling at the point.

[24] We calculated conditionally averaged currents over the inner shelf for the upwelling, relaxation, and convergent flow states (section 2, data analysis). This analysis complements the work of [*Dever*, 2004], who used drifter data to create average current fields for each flow state, but did not include data collected within 1.5 km of the coast. The conditionally averaged currents in Figure 3 reveal strikingly similar patterns on the inner shelf and mid-shelf, but there are also significant differences between the depth regimes.

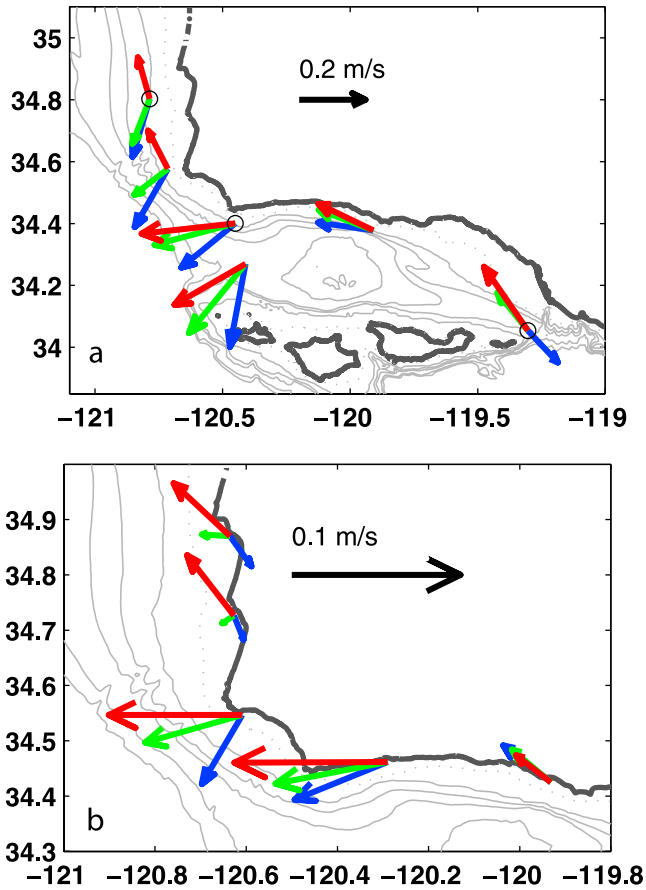

Figure 3. Near-surface current vectors on the mid-shelf and inner shelf, conditionally averaged by flow states (blue, upwelling; red, relaxation; green, convergence). (a) Mid-shelf currents from SIO moorings and HF radar. Currents measured at SIO moorings are marked with small circles; unmarked current vectors were measured by HF radar. (b) Inner-shelf currents at PISCO moorings. Current scale is consistent within each plot, but different between plots.

[25] Mid-shelf currents from surface HF radar measurements and 5-m SIO moored current meters show very consistent patterns (Figure 3a). At all locations, near-surface currents rotate clockwise between the upwelling, convergent, and relaxation flow states. This rotation amounts to a near-reversal of currents in the SMB upwelling zone, consistent with cycles of classical upwelling and relaxation. By contrast, conditionally averaged currents on the north shore of the SBC are always westward, and only slightly deflected by the different flow states. This is consistent with the predominantly cyclonic circulation in the channel.

[26] In the Santa Maria Basin, the response of the currents to the different flow states is quite different over the inner shelf and mid-shelf. Compare the two northernmost vector clusters over the mid-shelf (Figure 3a) with the analogous clusters over the inner shelf (Figure 3b). Over the mid-shelf, upwelling currents average about 0.15 ms^{-1} southwestward, significantly stronger than currents during relaxation. Inner-shelf currents during the upwelling flow state are highly variable, and the average current speed (0.01 ms^{-1}, northwestward) is only 10% of that observed over the mid-shelf. This change in cross shelf current speed is much greater than observed on the central California coast [*Lentz*, 1994]. The inner shelf responds more consistently to relaxation than to upwelling, with average currents up to 40% of the relaxation currents over the mid-shelf. The difference between upwelling and relaxation response is discussed in more detail in section 3.3.

[27] Currents at Arguello and Alegria (Figure 1) are strongly influenced by the flow convergence at Point Conception. Currents at these locations rotate according to flow state, with a larger southward component and smaller westward component for the equatorward and convergent flow states (Figure 3b). Near-surface currents at these locations average 0.07–0.09 ms^{-1}, westward during relaxation. These speeds are about 40% of the analogous currents observed at SMIN. Upwelling currents at Arguello and Alegria are slightly weaker, and about 30% of currents over the mid-shelf. This difference in transport is more consistent with prior studies [*Lentz*, 1994, 2001].

[28] Currents at Ellwood are unaffected by the upwelling and relaxation cycle. Average surface currents for each flow state are quite slow (0.025–0.033 ms^{-1}), and always westward, parallel to local bathymetry. Inner-shelf currents are about 20% of mid-shelf currents observed by HF radar.

3.2. Seasonal and Interannual Temperature Variability

[29] We discuss seasonal variations in wind, mid-shelf circulation state, and water temperatures over the inner shelf. For this analysis, winds from NDBC buoy 46062 and mid-shelf currents from SIO moorings SAMI and ANMI were run through a 3-week low-pass filter, and flow states were defined as by *Dever* [2004]. These data were compared with 3-week average temperatures over the inner shelf (Figure 4). We have chosen to use near-surface temperatures, which have the strongest seasonal variability. Mid-depth and near-bottom temperatures have weaker but similar patterns to those in Figure 4.

[30] The combined wind, current and temperature data reveal a standard seasonal pattern. Consistent with the southern California mystique, the waters near Point Conception experience a long spring, a longer summer, and a very short winter [*Brown*, 1966]. Superimposed on this cycle is some interannual variability consistent with the El Niño–La Niña cycle (http://www.cdc.noaa.gov/people/klaus.wolter/MEI).

[31] Spring upwelling raises cold water (<12°C) to the surface from March through May. Cold upwelled water is seen in the Santa Maria Basin (SMB) each year, but extends well into the Santa Barbara Channel (SBC) during a weak La Niña in 2002 and 2003. The equatorward flow state is seen over the mid-shelf during upwelling, and the flow patterns seem to suggest an equatorward advance of cold water. Closer examination (section 3.3) reveals that upwelling occurs at all locations simultaneously.

[32] In early summer, warm water (>15°C) is seen in the SBC, and there is a strong thermal gradient near Point Conception (between Jalama and Alegria). The warm water may extend well into the SMB in late summer, driven by poleward flow events. The poleward flow events are associated with weak poleward winds, and are presumably driven by the alongshore pressure gradient. The warmest

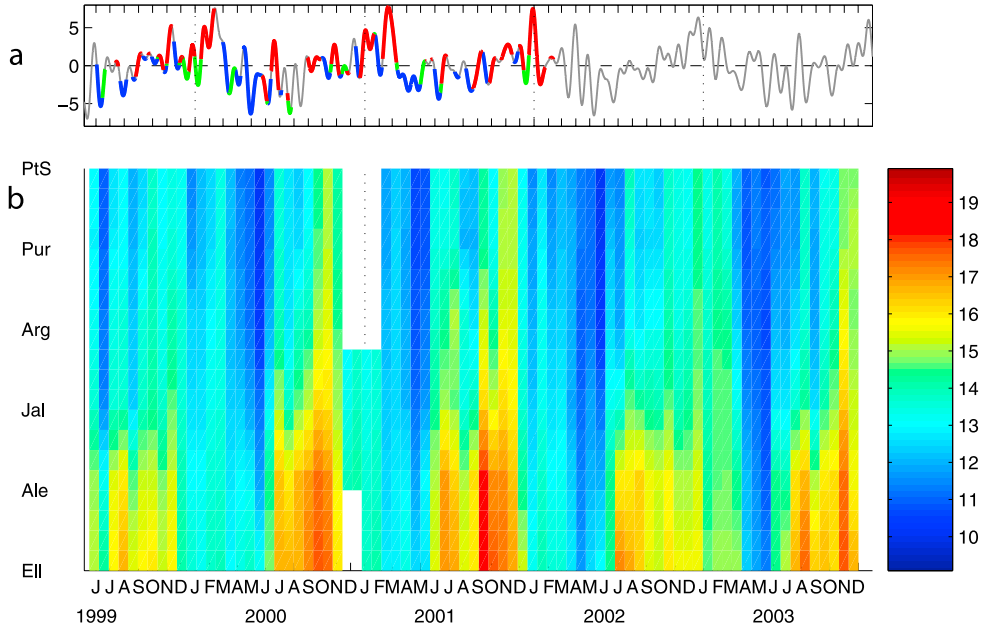

Figure 4. Winds, circulation condition, and near-surface inner-shelf temperatures for May 1999 through December 2003. In (a) Poleward component of wind measured at NDBC Buoy 46062. Line color indicates the synoptic flow state (blue, equatorward; red, poleward; green, convergent). (b) Inner-shelf temperatures as a function of time and along-shore location.

water (>19°C) and greatest northward extent of warm water were observed during a weak El Niño, in 2000 and 2001.

[33] There is a brief winter season, identified by cool water (13°–14°C) and weak temperature gradients throughout our study area. Winter storms drive strong poleward winds, which drive poleward currents in the SMB and SBC. Winter storms occur every year between January and March, and peak low-passed wind speeds appear to be independent of the El Niño–La Niña cycle. The higher occurrence of strong poleward winds in the spring of 2002 and 2003 may be related to large-scale climate cycles.

[34] The top to bottom temperature difference over the inner shelf varies with space and time. Temperatures from 3 m and 14 m depth were averaged over 2-week intervals for Figure 5. In mid-winter, there is little or no vertical stratification anywhere over the inner shelf. Average mid-summer stratification ranges between 1°C at Point Sal, the northernmost station, and 3°C at Ellwood (in 2003). The

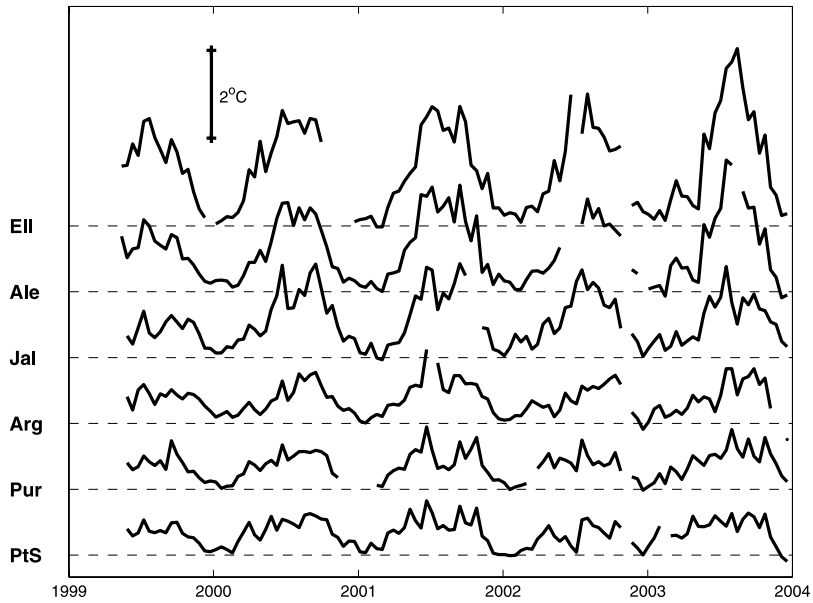

Figure 5. Near-surface to near-bottom temperature difference for complete data set, as function of time. Data from different stations are offset vertically, with the southeasternmost station, Ellwood, at the top.

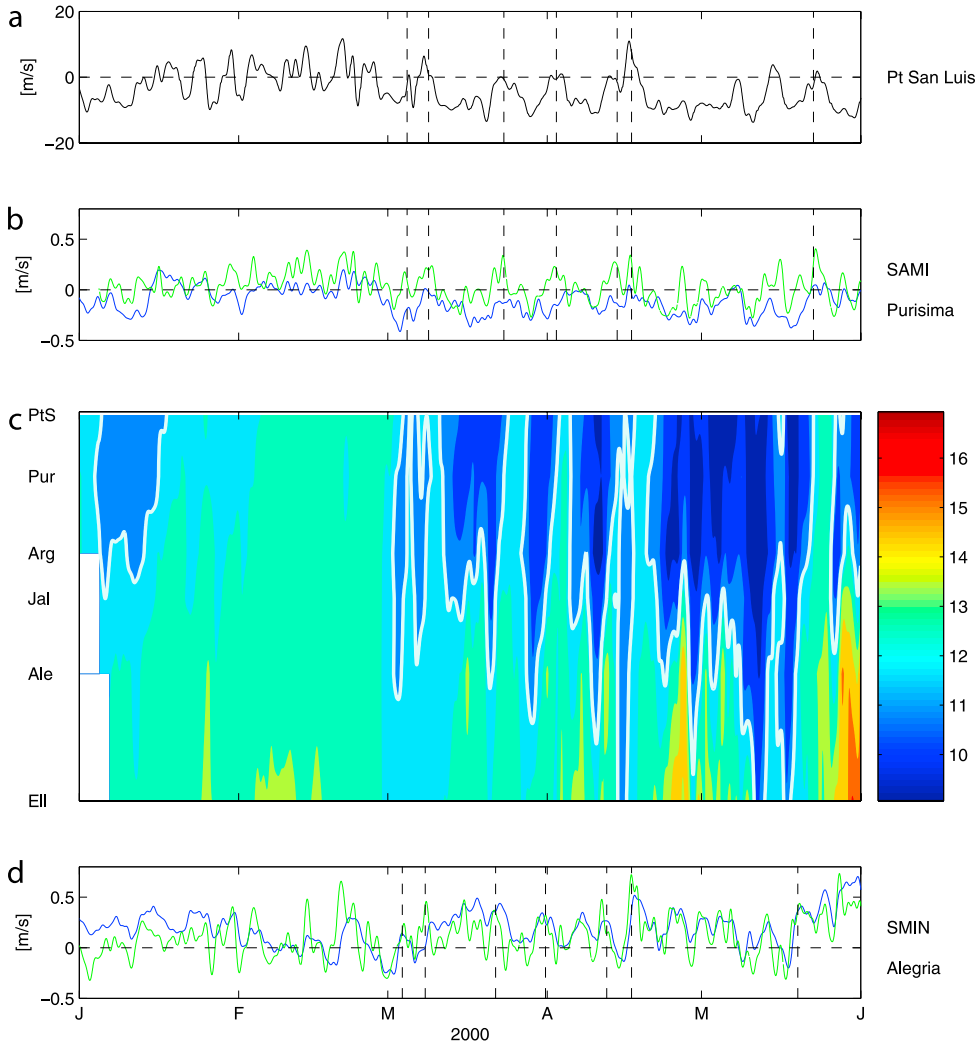

Figure 6. Winds, currents, and temperatures for January through May 2000. (a, b, d) Poleward components of winds and currents. Inner-shelf currents are exaggerated by a factor of 2. In Figure 6a, wind is measured at NDBC buoy 46023. In Figure 6b, currents are measured at SAMI (blue) and Purisima (green). In Figure 6d, currents are measured at SMIN (blue) and Alegria (green). Dashed vertical lines mark the start of relaxation events. (c) Near-surface temperatures over the inner shelf as a function of time and location. The 12°C isotherm is highlighted in white.

instantaneous top-to-bottom temperature difference can exceed 8°C (not shown). In our study area, salinity has at most an intermittent effect on stratification.

[35] This strong thermal stratification can decouple the top and bottom boundary layers, allowing strongly sheared cross-shelf transport, as discussed below (section 3.4). The strongest summer stratification in the Santa Barbara Channel is consistent with a buoyancy frequency over 15 cycles per hour. High-frequency internal waves (periods about 6–10 min) are frequently observed, the topic of a future paper.

3.3. Upwelling and Relaxation Cycles on the Inner Shelf

[36] We discuss inner-shelf temperatures and inner- and mid-shelf currents observed January through October 2000. On a meteorologic scale, the system cycles between upwelling and relaxation, but the responses of the water to the wind vary with location and time. The inner shelf and mid-shelf currents respond differently to wind relaxations, leading to significant cross-shelf shear in the Santa Maria Basin. Also, inner-shelf temperature distributions respond differently to upwelling and relaxation.

[37] Cold upwelled water appears over the inner shelf nearly simultaneously at all locations, but warm water propagates northward during relaxation events. This asymmetry is revealed by examination of the 12°C isotherm (white line in Figure 6c). During relaxation events (e.g., early April 2000) the isotherm tilts upward to the right, consistent with poleward propagation of warmer water. In contrast, during upwelling events, cooler water often appears simultaneously from Point Sal to Ellwood (e.g., late April 2000). In some upwelling events, cooling at Arguello even precedes cooling in the SMB (e.g., late March 2000); this is consistent with the upwelling center at Point Conception.

[38] During the upwelling season, wind relaxation events drive flow reversals over the inner shelf in the Santa Maria Basin. Relaxation events weaken the equatorward flow at

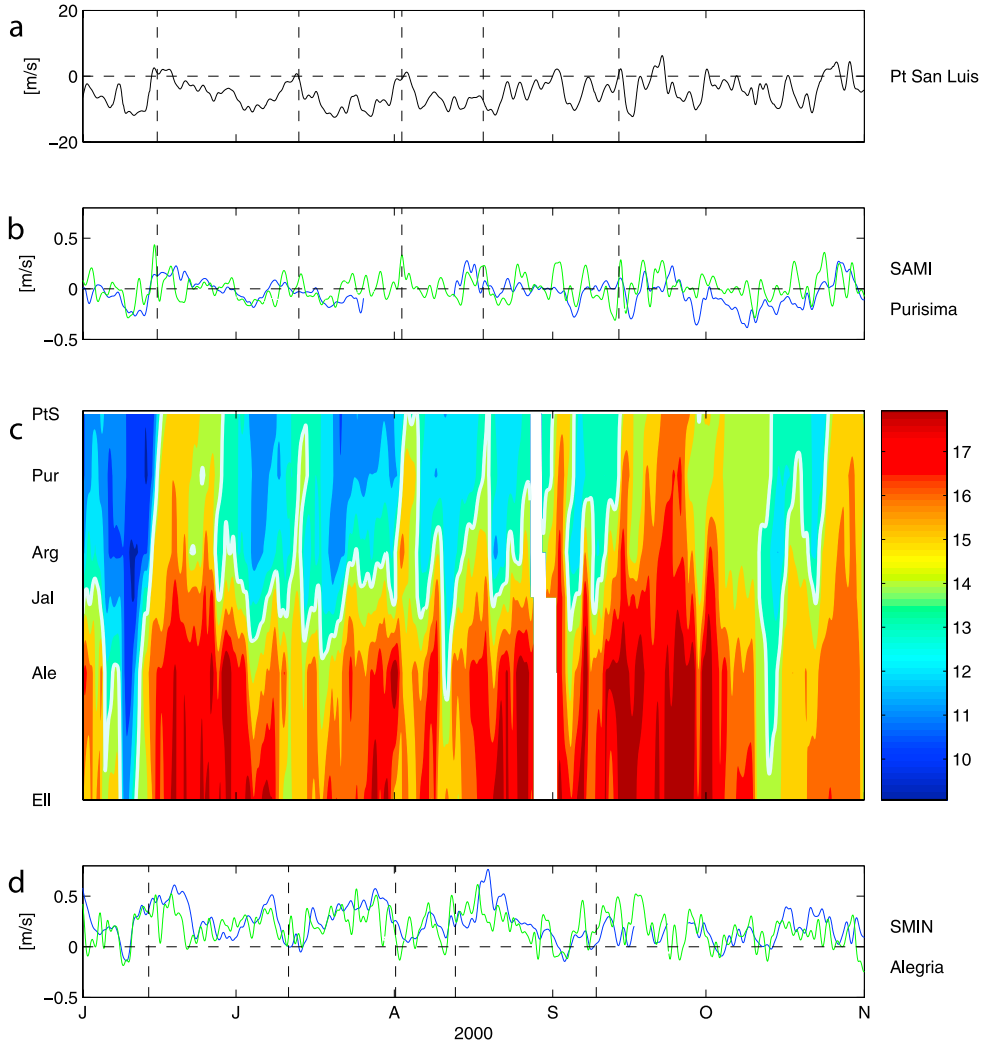

Figure 7. Winds, currents, and temperatures for June through October 2000. See caption for Figure 6. In Figure 7d, the 14°C isotherm is highlighted in white.

SAMI, but rarely cause mid-shelf current reversals (blue line in Figure 6b). By contrast, poleward currents are seen at Purisima (green line in Figure 6b) during several relaxation events. Poleward currents over the inner shelf drive along-shore advective transport of warm water. On several occasions (marked by dashed lines in Figure 6b), the 12°C isotherm (white line in Figure 6c) passes the Purisima mooring, accompanied by a peak in poleward currents. Flow reversals last from a few days to about a week, slightly longer in winter, and take 1 to 5 days to propagate from Jalama to Purisima.

[39] Currents in the western Santa Barbara Channel are poleward year round, owing to the along-shore pressure gradient that drives the SBC eddy. Inner shelf and mid-shelf currents are highly correlated; compare the currents at inner-shelf mooring Alegria and mid-shelf mooring SMIN (green and blue lines in Figure 6d). Again, we see evidence of the poleward propagation of warm water. When the 12°C isotherm passes Jalama, currents at SMIN and Alegria have poleward peaks (dashed vertical lines in Figure 6d).

[40] The patterns observed in winter 2000 continue into summer. The 14°C isotherm (highlighted in white in Figure 7c) has a sawtooth pattern, first tilting upward to the right during warming events then dropping nearly vertically when upwelling resumes. As in winter, the resumption of upwelling around Point Conception often precedes the appearance of cooler water at Purisima. When the 14°C isotherm passes Purisima, currents there turn poleward (times marked with vertical dashed lines in Figure 7b). During these events, mid-shelf currents at SAMI remain equatorward.

[41] A particularly strong poleward flow event coincided with abrupt relaxation of upwelling favorable winds in mid-June 2000. Before this event, cold water extended from Ellwood to Point Sal. Winds and currents were strongly equatorward in the Santa Maria Basin (Figures 7a and 7b) and weakly equatorward in the Santa Barbara Channel (Figure 7d). On 14 June the wind suddenly reversed, and a strong poleward flow event occurred over the inner shelf and mid-shelf, carrying warm water (up to 18°C) northward past Point Sal.

[42] The speed of isotherm motion over the inner shelf is comparable with the observed current speeds there. During the poleward flow event in mid-June, the 14°C isotherm traversed almost 100 km in 5 days, or ≈20 km d^{-1}. Inner-shelf currents at Alegria (≈0.2 ms^{-1}) were consistent with

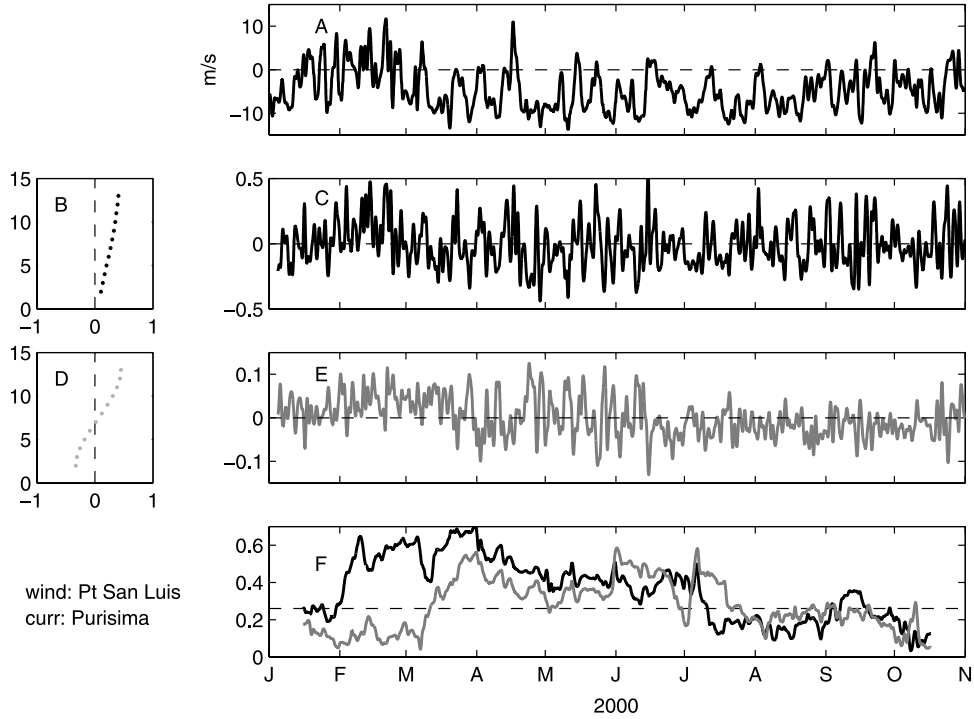

Figure 8. (a) Principal axis winds at NDBC buoy 46062 (ms^{-1} positive poleward). First EOF of along-shore currents at Purisima: (b) spatial part (plotted against meters above the bottom) and (c) temporal part (positive poleward). First EOF of cross-shore currents: (d) spatial part and (e) temporal part (positive onshore). (f) The 30-day running correlation between wind and first EOF of along-shore currents (black) and cross-shore currents (shaded). Horizontal dashed line is 95% confidence level.

this motion; mid-shelf currents at SMIN ($\approx$0.4 ms^{-1}) were significantly faster than needed to move the isotherm. These data suggest that heat is transported alongshore by advection over the inner shelf. Indeed, warming in the Santa Barbara channel, about 2°C per day, is roughly consistent with advective heat transport.

[43] The warm event moves into the Santa Maria Basin as a wedge, warming the inner shelf at Purisima about a day before warm water appears over the mid-shelf at SAMI and NDBC mooring 46023 (data not shown). Satellite images confirm the shape of the wedge. Mid-shelf currents associated with the warm water slow as it progresses; currents at SAMI are about half the speed of currents at SMIN.

3.4. Forcing of Inner-Shelf Circulation by Local Winds

[44] One might predict that inner-shelf currents in the Santa Maria Basin (in the California-Oregon upwelling zone) would be strongly correlated with local winds, and that currents in the Santa Barbara Channel (an upwelling shadow) would be weakly correlated with winds. Our analysis reveals that the correlations change with time, and between across-shelf and along-shelf currents.

[45] Along-shore currents at Purisima are driven by winds at NDBC 46062 during winter storms and spring upwelling. For the analysis in Figure 8, we use the first EOF of the along-shore current profile, containing 94% of the variance. Its spatial part is a sheared, unidirectional flow which decreases with depth (Figure 8b), and its temporal part (Figure 8c) clearly tracks the winds (Figure 8a). On the basis of a 30-day running correlation coefficient (dark line in Figure 8f), the temporal part of the first EOF is significantly correlated with the wind February through June, but the correlation suddenly decreases in late summer. This summer decorrelation between winds and alongshore currents occurred in every year we observed, 2000 through 2003.

[46] Across-shore currents at Purisima are correlated with local winds only during the upwelling season. The first EOF (60% of the variance) reveals a classic upwelling profile with offshore surface currents and onshore bottom currents during equatorward winds. The strong shear, observed over the inner shelf, is made possible by the strong thermal stratification discussed above (section 3.2). The temporal part of this EOF (Figure 8c) is clearly correlated with the wind during upwelling (March through June), but uncorrelated with the wind during the storm season (late summer, fall, and winter, Figure 8f, shaded line).

[47] Closer examination of the spring 2000 upwelling season (Figure 9) reveals strong cross-shelf shears in the wind and a cross-shelf divergence in transport. Ekman transport ($\tau/\rho_0 f$) is significantly stronger at NDBC buoy 46023 than at an SIO shore based meteorological station at Purisima (Figure 9b). Cross-shelf transport was estimated using currents measured at Purisma by assuming a 7-m surface layer thickness, based on the zero-crossing depth in Figure 8d, and at SAMI by assuming a 10-m surface layer thickness. Again, transport over the mid-shelf is significantly stronger than transport over the inner shelf.

[48] Winds at the shore and shelf locations are strongly correlated (r = 0.89), and inner-shelf transport is significantly correlated with shore winds (r = 0.63) and mid-shelf winds (r = 0.35). Currents over the mid-shelf at SAMI are

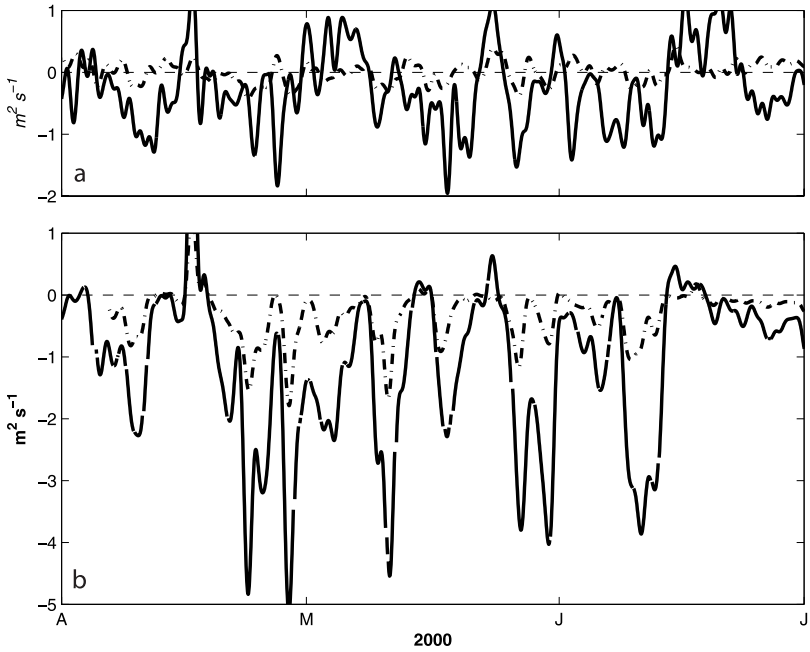

Figure 9. (a) Observed transport, assuming a 7-m layer thickness at inner-shelf station Purisima (dashed line) and a 10-m layer thickness at mid-shelf station SAMI (solid line). (b) Ekman transport based on winds from NDBC buoy 46023 (solid line) and an SIO shore-based meteorological station at Purisma (dashed line). Offshore transport is negative.

not significantly correlated with local winds, indicating that some process besides upwelling is affecting circulation there. The lack of correlation is apparent by inspection of Figure 9; significantly more onshore transport occurs at SAMI than would be predicted from the winds.

[49] Onshore transport occurs at inner-shelf station Purisima under three different wind conditions. Between 15 and 18 April, winds are poleward and transport is onshore. Between 27 and 28 May, winds at shore station Purisima are nearly slack, and transport is onshore. Finally, between 20 and 30 June, winds at Purisima and NDBC 46023 are weakly equatorward, and transport is still onshore (Figure 9). The wind/current correlation remains high during this period (Figure 8d). The persistent onshore transport over the inner shelf seems consistent with the persistent poleward transport discussed above.

[50] The north shore of the Santa Barbara Channel, especially in the eastern part, is sheltered from the wind, and currents over the inner shelf are generally uncorrelated with winds measured at mid-channel or on the shore. Currents at Ellwood, for example, are not significantly correlated with winds at any NDBC buoy, nor with winds measured on the shore near Ellwood (data not shown). During strong storms only, currents at Ellwood are correlated with local winds for up to a few days.

[51] In contrast with Ellwood, currents at Alegria are significantly correlated with winds through Gaviota Pass, which cuts through the Santa Ynez mountain range just north of Alegria. The principal axis of wind variability at the coast near Gaviota Pass is north-south (Figure 2a), nearly perpendicular to the principal axis of current variability at Alegria. The Gaviota wind time series (Figure 10a) is coherent with the winds in the Santa Maria Basin, showing some poleward wind events in January and February. However, the Gaviota time series is dominated by offshore (southward) winds, presumably blowing through Gaviota Pass.

[52] We compare the first EOFs of along-shore currents at Alegria (95% of variance, Figures 1b and 10c) and cross-shore currents (54% of variance, Figures 10d and 10e) with the cross-shore wind near Gaviota Pass. Along-shore currents at Alegria are significantly correlated with across-shore winds at Gaviota during winter only (dark line, Figure 10f). The across-shore currents, by contrast, are significantly correlated with cross-shore winds in a 30-day timescale over most of the year (light line, Figure 10f). These currents decorrelate from the wind in July of 2000, but are significantly correlated again in late summer. The vertical profile of the first EOF of the cross-shore currents is vertically sheared, but subtly different from the vertical profile at Purisima. Speeds in the upper layer increase steadily toward the surface. This pattern, and the correlation with offshore winds, suggest direct down-wind forcing of the cross-shore currents by local winds. A similar pattern of upwelling-like circulation driven by cross-shore winds instead of along-shore winds is observed at the Gulf of Tehuantepec in Mexico [e.g, *Martinez-Diaz-De-Leon et al.*, 1999]. Currents at Alegria are essentially uncorrelated with winds measured farther offshore in the SMB and SBC.

4. Conclusions and Discussion

[53] On temporal scales of months to years, circulation over the inner shelf in the Santa Barbara Channel (SBC) is generally consistent with currents observed over the mid-shelf and outer shelf in prior studies [e.g., *Hendershott and Winant*, 1996; *Auad and Hendershott*, 1997; *Harms and Winant*, 1998; *Dever et al.*, 1998; *Dorman and Winant*,

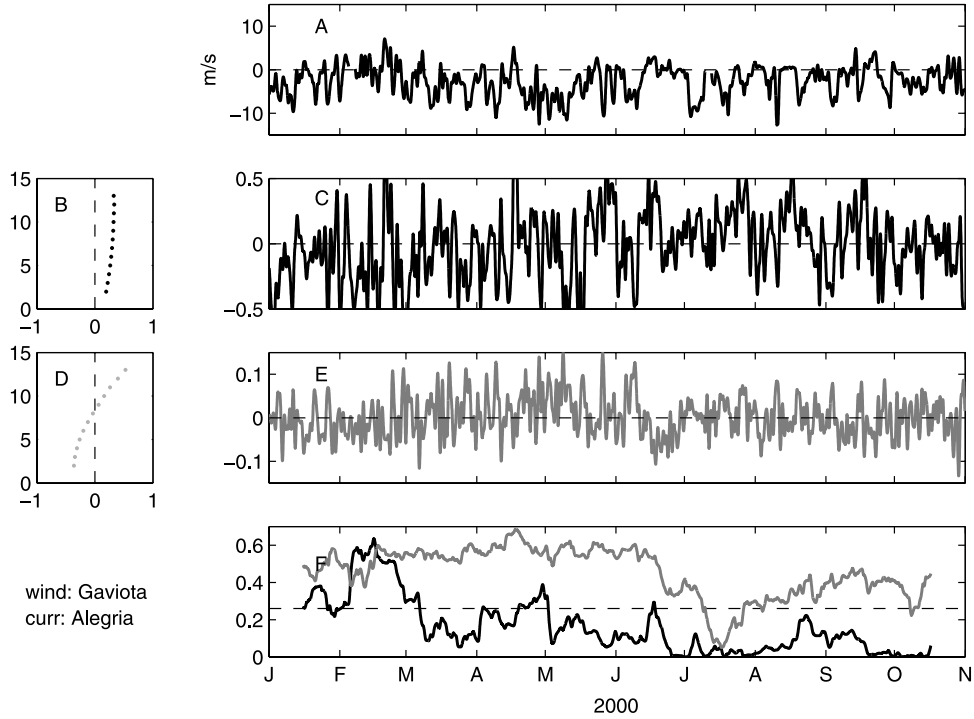

Figure 10. Same as Figure 8, but using winds from Gaviota, and currents from Alegria.

2000; *Winant et al.*, 2003; *Dever*, 2004]. Long-term average currents are poleward along the northern shore of the SBC, and inner-shelf current speeds are 20–40% of current speeds over the mid-shelf, consistent with *Lentz* [1995]. Changing wind and circulation patterns [*Dever*, 2004] have only a modest effect on the currents at the northern shore of the SBC. By contrast, average currents in the Santa Maria Basin (SMB) are equatorward over the mid-shelf and weakly poleward over the inner shelf. The difference is due to flow reversals that occur over the inner shelf during upwelling season.

[54] Synoptic-scale wind variations can have a more dramatic response over the inner shelf than over the mid-shelf. During relaxations of upwelling winds, equatorward flow over the mid-shelf of the SMB can coexist with poleward flow over the inner shelf. Poleward flow events lasting 1–5 days transport warm water from the SBC into the northern SMB. The warm water travels ~20 km d^{-1}, consistent with inner-shelf current speed. The warm currents may also carry drifting organisms, with ecological implications discussed below. By contrast with the poleward-traveling warm water observed during wind relaxation events, cold upwelled water appears simultaneously at all locations along the coast, indicating local upwelling.

[55] The correlation between winds and inner-shelf currents varies in time and space. Circulation at Purisima, in the SMB, is driven by along-shore winds, while circulation at Alegria, in the SBC, is driven by local cross-shelf winds at Gaviota Pass. At Purisima, along-shore currents are wind driven during winter storms and spring upwelling, but cross-shore currents are wind driven only during spring upwelling. At Alegria, cross-shore currents are wind driven in winter and spring, and along-shore currents are wind driven only in winter. In both locations, the current velocity component in the direction of the wind is significantly correlated with the wind from February through July of 2000, consistent with direct wind-driven currents.

[56] The wind-current correlation for all locations breaks down in mid-July of 2000. Similar analyses of all available data (1999 through 2002) suggest that this correlation breaks down between May and August each year, possibly owing to spatial gradients in wind stress. *Oey et al.* [2001] found that cyclonic circulation in the SBC is driven by a difference in wind stress between NDBC buoys 46053 and 46054, and *Beckenbach and Washburn* [2004] noted that the wind stress difference is greatest in summer. Spatial gradients in surface temperature are also greatest in summer.

[57] The area around Point Conception is a northern range boundary for many marine species with dispersing larvae; the range boundary for some species may due to the convergent mid-shelf circulation at Point Conception [*Gaylord and Gaines*, 2000]. Our results suggest that the existence of a flow-mediated range boundary may depend on the water depth where an organism spends its drifting stage. Organisms that drift over the mid-shelf may be strongly affected by the average mid-shelf circulation and therefore unable to move from the SBC into the SMB. Organisms drifting over the inner shelf, however, may be transported into the SMB during the poleward flow events described in this paper.

[58] **Acknowledgments.** This study builds on the extensive prior work of the Santa Barbara Channel–Santa Maria Basin Circulation study, funded by the Minerals Management Service and conducted by the Scripps Institution of Oceanography. J. Cordes of the Santa Barbara County Pollution Control Board provided a large meteorological data set, as did Clive Dorman of the Scripps Institution of oceanography. The National Data Buoy Center also provided meteorological data. The PISCO data were collected by C. Gottshalk and his hard-working team of technicians. The HF RADAR data were collected and processed by D. Salazar, B. Emery, and E. Beckenbach. This is contribution 173 from PISCO, the Partnership

for Interdisciplinary Studies of Coastal Oceans funded primarily by the Gordon and Betty Moore Foundation and David and Lucile Packard Foundation.

References

Atkinson, L., K. Brink, R. Davis, B. Jones, T. Paluskiewicz, and D. Stuart (1986), Mesoscale hydrographic variability in the vicinity of points Conception and Arguello during April–May 1983: The OPUS 1983 experiment, *J. Geophys. Res.*, *91*, 12,899–12,918.

Auad, G., and M. C. Hendershott (1997), The low-frequency transport in the Santa Barbara Channel: Description and forcing, *Cont. Shelf Res.*, *17*, 779–802.

Austin, J., and S. J. Lentz (2002), The inner shelf response to wind-driven upwelling and downwelling, *J. Phys. Oceanogr.*, *23*, 2171–2193.

Barth, J. A., and K. H. Brink (1987), Shipboard acoustic Doppler profiler velocity observations near Pt. Conception: Spring 1983, *J. Geophys. Res.*, *92*, 3925–3943.

Beckenbach, E. H., and L. Washburn (2004), Low-frequency waves in the Santa Barbara Channel observed by high-frequency radar, *J. Geophys. Res.*, *109*, C02010, doi:10.1029/2003JC001999.

Brink, K., and R. Muench (1986), Circulation in the Point Conception–Santa Barbara channel region, *J. Geophys. Res.*, *91*, 877–895.

Brown, B. (1966), *The Endless Summer* [movie], Image Entertainment, Chatsworth, Calif.

de Santis, M. (1985), *California Currents*, Presidio, Novato, Calif.

Dever, E. P. (2004), Objective maps of near-surface flow states near Pt. Conception, California, *J. Phys. Oceanogr.*, *34*, 444–461.

Dever, E. P., M. C. Hendershott, and C. D. Winant (1998), Statistical aspects of surface drifter observations in the Santa Barbara Channel, *J. Geophys. Res.*, *103*, 24,781–24,797.

Dorman, C. E., and C. D. Winant (2000), The structure and variability of the marine atmosphere around the Santa Barbara Channel, *Mon. Weather Rev.*, *128*, 261–282.

Ebbesmeyer, C. C., and W. J. Ingraham (1994), Pacific toy spill fuels ocean current pathways research, *Earth Space*, *7*, 7–9.

Emery, B., L. Washburn, and J. Harlan (2004), Evaluating radial current measurements from CODAR high frequency radars with moored current meters, *J. Atmos. Oceanic Technol.*, *21*, 1259–1271.

Gaylord, B., and S. D. Gaines (2000), Temperature or transport? Range limits in marine species mediated solely by flow, *Am. Nat.*, *155*, 769–789.

Gurgel, K. (1994), Shipborne measurement of surface current fields by HF radar, *L'Onde Electr.*, *74*, 54–59.

Harms, S., and C. Winant (1998), Characteristic patterns of the circulation in the Santa Barbara Channel, *J. Geophys. Res.*, *103*, 3041–3065.

Hendershott, M. C., and C. D. Winant (1996), Surface circulation in the Santa Barbara Channel, *Oceanography*, *9*, 114–121.

Large, W. G., and S. Pond (1981), Open ocean momentum flux measurements in moderate to strong winds, *J. Phys. Oceanogr.*, *11*, 324–336.

Lentz, S. J. (1994), Current dynamics over the northern California inner shelf, *J. Phys. Oceanogr.*, *24*, 2461–2478.

Lentz, S. J. (1995), Sensitivity of the inner-shelf circulation to the form of the eddy-viscosity profile, *J. Phys. Oceanogr.*, *25*, 19–28.

Lentz, S. J. (2001), The influence of stratificaion on wind-driven cross-shelf circulation over the North Carolina shelf, *J. Phys. Oceanogr.*, *31*, 2749–2760.

Limeburner, R. (Ed.) (1985), CODE-2 moored array and large-scale data report, *WHOI Tech. Rep. 85-35*, Woods Hole Oceanogr. Inst., Woods Hole, Mass.

Martinez-Diaz-De-Leon, A., I. Robinson, D. Ballestero, and E. Coen (1999), Wind-driven ocean circulation features in the Gulf of Thuantepec, Mexico, revealed by combined SAR and SST satellite sensor data, *Int. J. Remote Sens.*, *20*, 1661–1668.

Muenchow, A. (2000), Wind stress curl forcing of the coastal ocean near Point Conception, California, *J. Phys. Oceanogr.*, *30*, 1265–1280.

Oey, L.-Y., D.-P. Wang, T. Hayward, C. Winant, and M. Hendershott (2001), "Upwelling" and "cyclonic" regimes of the near-surface circulation in the Santa Barbara Channel, *J. Geophys. Res.*, *106*, 9213–9222.

Pineda, J. (2000), Linking larval settlement to larval transport: Assumptions, potentials, and pitfalls, in *Oceanography of the Eastern Pacific*, vol. 1, edited by J. Farber-Lorda, pp. 84–105, Cent. de Invest. Cient. y Educ. Super. de Ensenada, Ensenada, Mexico.

Smith, R. L. (1995), The physical processes of coastal ocean upwelling systems, in *Upwelling in the Ocean: Modern Processes and Ancient Records*, edited by C. P. Summerhayes et al., pp. 39–64, John Wiley, Hoboken, N. J.

Strub, P., J. S. Allen, A. Huyer, R. L. Smith, and R. C. Beardsley (1987), Seasonal cycles of currents, temperatures, winds and sea level over the northeast Pacific continental shelf: 35°N to 48°N, *J. Geophys. Res.*, *92*, 1507–1526.

Valentine, J. W. (1966), Numerical analysis of marine molluscan ranges on the extratropical northeastern Pacific shelf, *Limnol. Oceanogr.*, *11*, 198–211.

Wares, J., S. D. Gaines, and C. Cunningham (2000), A comparative study of asymmetric migration events across a marine biogeographic boundary, *Evolution*, *55*, 295–306.

Winant, C., E. Dever, and M. Hendershott (2003), Characteristic patterns of shelf circulation at the boundary between central and southern California, *J. Geophys. Res.*, *108*(C2), 3021, doi:10.1029/2001JC001302.

C. N. Cudaback, Department of Marine, Earth and Atmospheric Sciences, North Carolina State University, Campus Box 8208, Raleigh, NC 27695-8208, USA. (cynthia_cudaback@ncsu.edu)

E. Dever, College of Oceanic and Atmospheric Sciences, Oregon State University, 104 COAS Administration Building, Corvallis, OR 97331-5503, USA. (edever@coas.oregonstate.edu)

L. Washburn, Institute for Computational Earth Systems Science, University of California, Santa Barbara, Santa Barbara, CA 93106, USA. (washburn@icess.ucsb.edu)